

RELIABILITY ANALYSIS METHOD FOR BURIED PIPELINE UNDER THAWING LANDSLIDE OF FROZEN SOIL

Xiaoben Liu*, Han Zhang*, Yue Yang*, Dong Zhang*, Bolati Dinaer and Hong
Zhang***

* National Engineering Laboratory for Pipeline Safety, MOE Key Laboratory of Petroleum Engineering, Beijing
Key Laboratory of Urban Oil and Gas Distribution Technology, China University of Petroleum-Beijing, 102249,
Beijing, China.

e-mails: xiaobenliu@cup.edu.cn, zhanghan7131@163.com, yangyue6679@163.com, zhangdongcup@163.com,
hzhang@cup.edu.cn

** PipeChina West Pipeline Company, Xinjiang Urumqi, 830000, China.
e-mail: dinaerbolati@163.com

Keywords: Frozen soil; Thawing landslide; Buried Pipelines; Monte Carlo; Reliability analysis.

Abstract. *The petroleum pipeline passing through permafrost region is faced with thawing landslide geological hazards, which seriously affects the safety of the pipeline operation. In the research, the maximum axial strain of the pipe under the thawing landslide is calculated by theoretical analytical method. The ultimate tensile and compressive strains of the pipe are calculated and the ultimate state equation of pipe based on strain is established. The failure probabilities of pipe under tensile failure and compressive buckling subjected to thawing landslide were calculated by Monte Carlo method. The critical displacements of thawing landslide under different conditions were given based on the quantitative reliability analysis. This research demonstrated that compared with increasing pipe wall thickness and decreasing internal operating pressure, decreasing ultimate resistance of soil has a more significant effect on increasing critical displacement. The research provides a reference for the safe operation of long distance transportation pipeline by structural reliability quantitative analysis of pipeline passes through the permafrost zone.*

1 INTRODUCTION

The pipeline crossing the soil thermal thawing slip slope longitudinally is mainly subject to axial forces, and the uphill pipeline is susceptible to tensile failure and downhill pipeline is susceptible to buckling instability. Therefore, many scholars have studied the reliability of pipelines under axial loads. Wijewickreme [1] analyzed the failure probabilities of pipelines subjected to longitudinal ground motion. Nobahar [2] conducted a reliability analysis of pipelines subjected to soil motion caused by ice planing and concluded that the final ultimate state of the pipeline was compressional local buckling. Alvarado-Franco [3] simulated the probability of landslide occurrence and failure probabilities at each point of the pipe by Monte Carlo method and proposed a simple and efficient quantitative model for evaluating the failure probabilities of pipe due to landslide interactions. Combined with LS-DYNA finite element software the ultimate state equation of yield strength and maximum effective impact stress was established by Youlv Li [4] to calculate the failure probabilities of the pipe. Based on the Von Mises criterion, an ultimate state equation based on stress was established by Xiaolei Ma [5] to calculate the reliability of the pipeline under external impact load by Monte Carlo method. Zhou.W [6] analyzed the pipeline reliability under tensile and compressive subjected to thaw slumping load, calculated the strain of the pipe by the analytical method of Rajani [7] and Yoosef-Ghods [8], establishing ultimate state equation based on strain, and calculating the failure probabilities of the pipe under landslide by Monte Carlo method.

Pipelines crossing slopes longitudinally are usually chosen in engineering application because of it is safer than the pipelines crossing slopes transversely. But the problems about the reliability of pipelines crossing the thermal thawing slip slope longitudinally are yet to be analyzed in the China-Russia Crude Oil Pipeline, and there are few studies about the reliability of oil and gas pipelines under soil axial displacement. Therefore, this paper calculated the failure probabilities of pipelines under the thawing landslide by Monte Carlo method, and analyzed the effects of pipeline operating internal pressure, pipe wall thickness and soil ultimate resistance on the pipeline reliability quantitatively.

2 ULTIMATE STATE EQUATION BASED ON STRAIN AND PARAMETER DISTRIBUTIONS FOR PIPELINES

2.1 Establishment of ultimate state equation

Considering the parameters affecting the reliability of pipelines under thermal thawing slip as the strain capacity and the maximum axial strain, the ultimate state equations based on strain are developed for the tensile and compressive sections of the pipe, respectively.

$$\begin{cases} g_1(x) = \text{TSC} - \varepsilon_t^{\max} \\ g_2(x) = \text{CSC} - \varepsilon_c^{\max} \end{cases} \quad (1)$$

Where, TSC and CSC are the tensile strain capacity and compressive strain capacity of the pipe. ε_t^{\max} and ε_c^{\max} are the maximum axial tensile strain and the maximum axial compressive strain. According to the theory of structural reliability, the pipeline is safe when $g_1(x) > 0$ and $g_2(x) > 0$. When $g_1(x) < 0$, the pipeline is damaged due to tension, and when $g_2(x) < 0$, the pipeline is destabilized due to compressive buckling. The strain capacity is calculated by CSA Z662 model [9], while the maximum axial strain is obtained by the theoretical analytical method.

(1) Tensile Strain Capacity (TSC)

In different standards the tensile strain capacity has different calculation models, among which the tensile strain capacity model in CSA Z662-07 [9] is simpler. Assuming the weld defect is surface type, the tensile strain capacity calculation model in CSA Z662-07 [9] is used.

$$\varepsilon_t^{cri} = \delta^{(2.36-1.58R_{YT}-0.101\xi\eta)} (1+16.1R_{YT}^{-4.45}) (-0.157+0.239\xi^{-0.241}\eta^{-0.315}) \quad (2)$$

Where, ε_t^{cri} is the tensile strain capacity of the pipe, %; R_{YT} is the pipe yield ratio, in the range 0.7 ~ 0.9; δ is the apparent toughness, mm, in the range 0.1 ~ 0.3 mm; ξ is the ratio of the height of the weld defect to the pipe wall thickness, in the range 0 ~ 0.5; η is the ratio of the length of the weld defect to the pipe wall thickness, in the range 1.0 ~ 10.0.

(2) Compressive Strain Capacity (CSC)

The compressive strain capacity is calculated by the University of Alberta's UOA-2001 model [10] for a glossy tube with a stress-strain curve with a yield plateau, which is fitted with finite element data to obtain.

$$\varepsilon_c^{cri} = 40.4 \left(\frac{t}{D}\right)^2 (1-0.906f_p)^{-1} \left(\frac{E_1}{\sigma_y}\right)^{0.8} \left[1.12 - \left(\frac{h_g}{t}\right)^{0.15}\right] \quad (3)$$

Where, ε_c^{cri} is the compressive strain capacity, %; D is the outer diameter of the pipe, mm; t is the pipe wall thickness, mm; f_p is the internal pressure coefficient; h_g is the outer surface of the pipe wave defects peak to valley height, mm; E_1 is the modulus of elasticity, GPa; σ_y is the longitudinal yield strength of the pipe, MPa.

(3) Pipeline maximum axial strain calculation model

The side view of the pipeline under thermal thawing slip is shown in Figure 1, where the pipeline crosses the slope in the shape of the letter “Z”, in which the section BC of the pipe crosses the unstable soil (thermal thawing slip area), and the section AB and CD and horizontal pipes at both ends of the slope are laid in the stable soil. The points A and D are infinite distant ends, and the length of section BC is L . The horizontal pipe sections are connected with the slope pipe sections by bends, and the angle of the slope is θ .

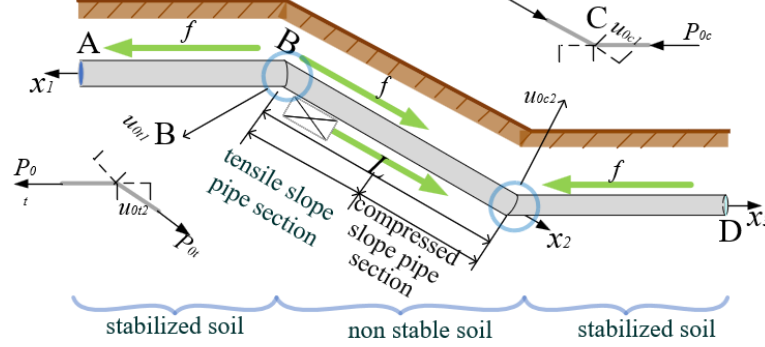


Figure 1: Pipeline under the action of soil thermal thawing slip [6].

The model of strain analysis of pipe under landslide proposed by Rajani [7] and improved by Yoosef-Ghodsi [8] and Zhou.W [6] is used to solve the axial strain of the pipe. The model assumes that the pipe is subjected to minimal bending, and the mainly subjected to the axial force P_0 generated by the slip and the frictional force between the pipe and the soil, and the frictional force per unit length of the pipe is f . The BC section also has the component $qs\sin\theta$ of the pipe's own gravity q along the axial direction. Tensile strain is generated in the uphill pipe due to tension. Compressive strain is generated in the downhill pipe due to compression. Therefore, the maximum axial tensile strain is located at point B and the maximum axial compressive strain is located at point C.

According to the assumptions of Zhou.W [6], the axial force of the slope pipe is assumed to be equal to that of the horizontal pipe. The displacement of point B at the top of the slope pipe u_{0t1} is due to the axial tension P_{0t} , and the horizontal displacement of point B at the horizontal pipe is u_{0t2} ; the displacement of the bottom point C u_{0c1} is due to the axial compression P_{0c} , and the horizontal displacement of point C is u_{0c2} .

The axial force P_0 (P_{0t} , P_{0c}) of the pipeline described above is due to the slip, which does not include the initial axial force P_0^{init} generated by the Poisson effect and the temperature difference between the operation and installation. The total axial force of the pipe is σ_1^{total} , $P_0=A(\sigma_1^{total}-\sigma_1^{init})$; where A is the sectional area of the pipe. Therefore, when the pipe yields, the ultimate axial force in tension and compression are:

$$\begin{cases} P_{yt} = A(\sigma_{1y}^t - \sigma_1^{init}) \\ P_{yc} = A(\sigma_{1y}^c - \sigma_1^{init}) \end{cases} \quad (4)$$

Where, σ_1^{init} is the initial stress of the pipe, MPa; σ_{1y}^t is the axial tensile stress at yield of the pipe, MPa; σ_{1y}^c is the axial compression stress at yield of the pipe, MPa. the initial stress of the pipe is $\sigma_1^{init}=\nu\sigma_h-E_1\alpha\Delta T$, ν is the Poisson's ratio; α is the temperature stress coefficient; ΔT is the temperature difference, °C; σ_h is the hoop stress of the pipe, $\sigma_h=\frac{p(D-2t)}{2t}$, p is the internal pressure of the pipe, MPa. σ_{1y}^t and σ_{1y}^c can be derived from the bilinear stress-strain model of the material [8], and the fourth strength theory [8] failure determination.

$$\begin{cases} \sigma'_{1y} = \frac{1}{2}(\sigma_h + \sqrt{4\sigma_y^2 - 3\sigma_h^2}) \\ \sigma^c_{1y} = \frac{1}{2}(\sigma_h - \sqrt{4\sigma_y^2 - 3\sigma_h^2}) \end{cases} \quad (5)$$

The top view of the pipe crossing the thermal thawing slip slope longitudinally is shown in Figure 2, the displacements of the horizontal pipe at the infinitely distant ends of points A and D are 0. The displacements of the points B and C in the horizontal direction are converted into displacements in the slope direction, assuming that the slip slope displacement u_{total} is equal to the geometric elongation produced by the pipe being pulled in the slope direction and the geometric compression produced by the pipe being compressed in the slope direction.

$$\begin{cases} u_{total}(P_{0r}) = u_{0r1}(P_{0r}) + u_{0r2}(P_{0r}) \cos \theta \\ u_{total}(P_{0c}) = u_{0c1}(P_{0r}) + u_{0c2}(P_{0r}) \cos \theta \end{cases} \quad (6)$$

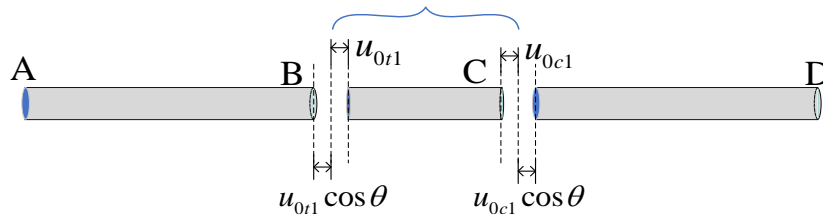


Figure 2: Top view of the pipe crossing the thermal thawing slip slope longitudinally.

Thus, the equation between the axial force and the amount of thermal thawing slip of point B and C can be solved. In this study, the ideal elastoplastic model used by Rajani [7], O'Rourke [11] was used to describe the pipe-soil interaction relationship as follows.

$$\begin{cases} f = \pi D k_x u & (|u| \leq u_x) \\ f = \pi D k_x u_x = F_x & (|u| \geq u_x) \end{cases} \quad (7)$$

Where u is the relative axial displacement of the pipe and soil, mm; u_x is the relative axial displacement of the pipe and soil when the soil yields, mm; F_x is the ultimate soil resistance per unit length of pipe, N/mm; k_x is the axial road base modulus of the soil, N/mm³. The pipe gravity is neglected since it's much smaller than the soil friction. The control equation of the pipe can be obtained according to the ideal elastoplastic model, the equilibrium equation of elastoplastic mechanics and geometric equations. When the soil is elastic, the control equation is:

$$\frac{d^2 u}{dx^2} - \frac{k_x u \pi D}{EA} = 0 \quad (8)$$

Where, E is modulus of pipe, MPa, when the pipe is elastic, E_1 is the elastic modulus, when the pipe is plastic E_2 is the plastic modulus (E_2^t when tension, E_2^c when compression). When the soil is elastic, the generalized solution is

$$u = k_1 e^{\lambda x} + k_2 e^{-\lambda x} \quad (9)$$

Where, $\lambda = (k_x \pi D / EA)^{1/2}$, k_1 and k_2 are TBD factor. When the soil is plastic, the control equation is:

$$dN = \pi D k_x u_x \cdot dx \quad (10)$$

The broad interpretation is:

$$u = \frac{F_x}{2EA}x^2 + k_3x + k_4 \quad (11)$$

Where, k_3 and k_4 are TBD factor. The unstable soil transitions from elastic to plastic with the displacement of unstable soil increases, while the stable soil remains elastic; if the displacement of unstable soil is greater, the stable soil also gradually enters the plastic stage. Therefore, the strain distribution function of the pipe is solved in 3 stages:

① Stage 1: both soil and pipe are elastic

As shown in the first case in Figure 3, the left pipe is located in the stable soil, the right pipe is located in the unstable soil, both stable soil and unstable soil are regarded as semi-infinite length of elastic soil. At this point, the boundary conditions are: $u_{1(x=+\infty)}=0$; $\varepsilon_{1(x=0)}=P_{0t}/E_1A$. Combined with the geometric equations to solve the displacement of the horizontal pipe B point is $u_{0t2}=P_{0t}/E_1A\lambda$. Similarly, the displacement at point C of the horizontal pipe is $u_{0c2}=P_{0c}/E_1A\lambda$.

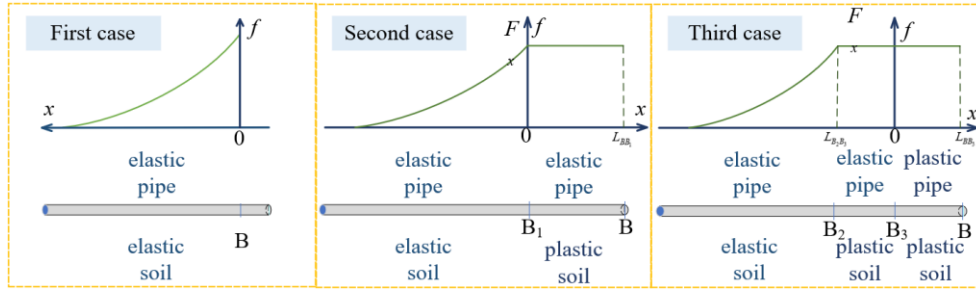


Figure 3: Reaction force of soil distribution in the tensioned section of the pipe.

② Stage 2: part of the soil enters the plastic stage and the pipe remains in elastic stage

As shown in the second case in Figure 3, $x=0$ is the point B_1 , $x=L_{BB1}$ is the point B. The stable soil in elastic stage in $x \leq 0$, the stable soil in plastic stage in $0 < x \leq L_{BB1}$. The soil at point B is the first to reach the elastic-plastic boundary, at this time $u_{0t2}=u_x$, and the critical axial force of point B is $P_{0t}^{cri1}=E_1A\lambda u_x$. After $u_{0t2} > u_x$ the stable soil near point B starts to enter the plastic stage, while the distal end is still in the elastic stage, the length of the plastic stage of the stable soil is $L_{BB1}=(P_{0t}-P_{0t}^{cri1})/F_x$.

The boundary conditions are $u_{1(x=-\infty)}=0$; $u_{1(x=0)}=u_x$; $\varepsilon_{1(x=L_{BB1})}=P_{0t}/E_1A$. Combining the geometric equations, $u_{0t2}=(P_{0t}^2-(P_{0t}^{cri1})^2)/2E_1AF_x+u_x$. Similarly, the critical axial force at point C is $P_{0c}^{cri}=-|E_1S\lambda u_x|$, the displacement of point C is $u_{0c2}=(P_{0c}^2-(P_{0c}^{cri})^2)/2E_1AF_x+u_x$.

③ Stage 3: the pipe and part of the soil enters the plastic stage

As shown in the third case in Figure 3, $x=0$ is the point B_3 , $x=-L_{B2B3}$ is the point B_2 , $x=L_{BB3}$ is the point B. The stable soil in elastic stage in $x \leq -L_{B2B3}$, the stable soil in plastic stage in $-L_{B2B3} \leq x \leq -L_{BB3}$. The pipeline is in elastic stage in $x \leq 0$; pipeline in plastic stage in $0 \leq x \leq L_{BB3}$.

The soil at point B is the first to reach the elastic-plastic boundary, at this time $P_{0t}=P_{yt}$, and the critical axial force of point B is $P_{0t}^{cri2}=P_{yt}$. After $P_{0t} > P_{yt}$ the stable soil near point B starts to enter the plastic stage, while the distal end is still in the elastic stage, the length of the plastic stage of the stable soil is $L_{BB3}=(P_{0t}-P_{yt})/F_x$.

Now, the boundary conditions are $\varepsilon_{1(x=L_{BB3})}=P_{0t}/E_2A+P_{yt}/E_1A-P_{yt}/E_2A$; $u_{1(x=-\infty)}=0$; $u_{1(x=-L_{B2B3})}=u_x$; $u_{1(x=0)}=u_{0t3}$. The displacement of point B of the uphill horizontal pipe is $u_{0t2}=P_{0t}^2/2E_2AF_x+(1/E_2-1/E_1)(P_{0t}^{cri2}-2P_{0t})P_{0t}^{cri2}/2AF_x+u_x/2$.

Similarly, the critical axial force of point C is $P_{0c}^{cri2}=P_{yc}$, the displacement of point C is $u_{0c2}=P_{0c}^2/2E_2AF_x+(1/E_2-1/E_1)(P_{0c}^{cri2}-2P_{0c})P_{0c}^{cri2}/2AF_x+u_x/2$.

In summary, $u_{0t1}=u_{0t2}$; $u_{0c1}=u_{0c2}$ according to the symmetry.

When the soil transitions from the elastic to the plastic state, the frictional force per unit length of the slope pipe reaches the ultimate resistance F_x , the axial force at point B of the slope pipe is $P_{0t}=P_{0t}^{max}$, the axial force at point C is $P_{0c}=P_{0c}^{max}$. The axial force equilibrium equation of the slope pipe is as follows.

$$P_{0t}^{max} + P_{0c}^{max} = F_x L \quad (12)$$

Since the amount of thermal thawing slip is the same at this time on the upper and lower slopes, $u_{total}(P_{0t}^{max})=u_{total}(P_{0c}^{max})$, the equation can be solved to obtain P_{0t}^{max} , P_{0c}^{max} and the critical displacements of thawing landslide u_s^{cri} when the soil reaches plasticity.

Given a soil thermal thawing slip, when $u_s < u_s^{cri}$, $u_{total}(P_{0t})=u_{total}(P_{0c})$. The axial force at two points B and C (P_{0t} and P_{0c}) of the slope pipe can be obtained by the relationship between the axial force of the pipe and the thermal thawing slip; when $u_s \geq u_s^{cri}$ soil has entered the plastic stage, at this time axial force of B and C reached the maximum P_{0t}^{max} and P_{0c}^{max} respectively, make $P_{0t}=P_{0t}^{max}$, $P_{0c}=P_{0c}^{max}$. Finally, the maximum axial strain of the pipe can be obtained by combining the constitutive equation, the geometric equation and the relationship between the axial force of the pipe and the thermal thawing slip.

2.2 Parameters distribution and values for pipeline reliability analysis

Many scholars [6, 12] considered diameter, wall thickness, and internal pressure of the pipe obeyed normal distribution, and the standard deviation of each parameter was derived by combining the Lajda criterion [13] and the relevant standards. The Lajda criterion [13] considers the standard deviation $\Delta x=3\delta$, indicates that the values are distributed in $[\mu+\Delta x, \mu-\Delta x]$, where, μ is the mean value; δ is the standard deviation; Δx is the standard deviation. Many scholars use the coefficient of variation COV to characterize the degree of uncertainty, dispersion of random variables, which is related to the mean and standard deviation:

$$COV=\delta / \mu \quad (13)$$

Δx can be obtained from the relevant standards, GB/T9711-2017 “Steel pipes for transmission in pipeline systems of oil and gas industry” [14] stipulates that the deviation of pipe diameter for welded pipes with diameter between 610 mm and 1422 mm is 0.005D and the maximum shall not exceed 4.0 mm, while the deviation of pipe wall thickness is 0.1t when the wall thickness is between 5 mm and 15 mm, and the deviation is 1.5 mm when it is greater than 15 mm. therefore, the standard deviations of diameter and wall thickness are 1.33 and 0.42, respectively. for the internal pressure distribution law of the pipe, Caley [15], Sun Chunmei [16] and others considered that the coefficient of variation of the pressure distribution is 0.1, and then the standard deviation is 0.58 when the internal pressure is 5.80 MPa. According to Zhou W. [6], the law of the ultimate soil resistance F_x per unit length distribution is set as a lognormal distribution. In this paper, COV is 0.05, δ is 3.83. Behrooz Keshtegar [17] considered that COV of the yield strength of pipe is 0.07, and its δ is 31.5. Combining the relevant criteria the distribution and values of the parameters are shown in Table 1. In Table 1, F_y is the tensile strength of the pipe.

2.3 Pipeline ultimate state reliability index

In CSA Z662 [9], the ultimate state reliability index of a pipeline is defined as a function of pipeline diameter, pressure and population density. The population density of the China-Russia Crude Oil Pipeline is taken as 0, the reliability index R_T is calculated as 0.999. Although the Daxinganling is sparsely populated, it is one of the important forestry bases in China as a

primitive forest, therefore this paper takes 10^{-4} as the maximum failure probability to ensure the safe operation.

Table 1: Distribution and values of parameters for pipeline reliability analysis.

Parameters	Unit	Distribution law	Mean value μ (base case value)	Standard deviation δ	Source
D	mm	Normal distribution	813	1.33	GB9711-2017
t	mm	Normal distribution	12.7	0.42	GB9711-2017
p	MPa	Normal distribution	5.8	0.58	Caleyo、Sun, Chunmei et al.
F_x	N/mm	Log-normal distribution	76.62	3.83	Zhou W.
σ_y	MPa	Normal distribution	450	31.5	Behrooz Keshtegar et al.
L	m	Determine	500	—	—
θ	°	Determine	20	—	—
u_s	mm	Determine	10~1000	—	—
f_p	—	Determine	0.4	—	—
F_y	MPa	Determine	535	—	—
R_{YT}	—	Determine	0.84	—	—
ν	—	Determine	0.3	—	—
E_1	GPa	Determine	205	—	—
E_{2t}	MPa	Determine	6150	—	—
E_{2c}	MPa	Determine	6150	—	—
ΔT	°C	Determine	20	—	—

3 PIPELINE RELIABILITY ANALYSIS METHOD UNDER THE THERMAL THAWING SLIP

3.1 Calculation process of pipeline failure probability under thermal thawing slip

(1) Calculation process of failure probability

Tensile damage and compression buckling of the pipe are interrelated. When the maximum axial tensile strain reaches the TSC first, the pipe will under tensile failure; when the maximum axial compressive strain reaches the CSC first, the pipe will have a buckling failure. As shown in Figure 4, making the maximum axial tensile strain of the pipe is equal to the TSC, i.e. $\varepsilon_t^{max} = \varepsilon_t^{cri}$, and the maximum axial compressive strain of the pipe is equal to the CSC, i.e. $\varepsilon_c^{max} = \varepsilon_c^{cri}$. The relationship between the axial force of the pipe and the amount of thermal thawing slip is used to back calculate the soil thermal melt slip u_t^{cri} for tensile damage of the pipe and the soil thermal melt slip u_c^{cri} for compression buckling of the pipe.

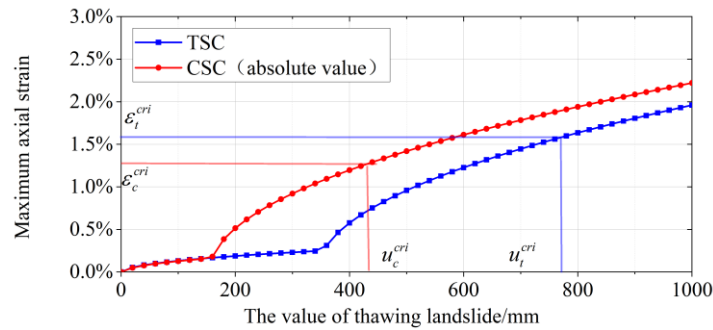


Figure 4: Critical displacements of thawing landslide.

The pipeline failure probability was calculated by MATLAB to perform 10^6 simulations, i.e., the process in Figure 5 was performed one million times to obtain one million u_t^{cri} , u_c^{cri} and u_s^{cri} . The pipeline failure probability calculation process is shown in Figure 6.

① When $u_t^{cri} \leq u_c^{cri}$ and $u_t^{cri} \leq u_s^{cri}$, the failure form is tensile failure, and the number of tensile failure times is recorded as N_i ; at this time, when $u_t^{cri} \leq u_s$ the number of times a pipe under tensile

failure is recorded as n_t . ② When $u_c^{cri} \leq u_t^{cri}$, and $u_c^{cri} \leq u_s^{cri}$, the failure form is compressive buckling, and the number of compressive buckling times is recorded as N_c ; at this time, when $u_c^{cri} \leq u_s$ the number of times a pipe under compressive buckling is recorded as n_c . ③ When $u_c^{cri} > u_t^{cri}$ and $u_c^{cri} > u_s^{cri}$, the pipe can neither be damaged in tension nor buckled in compression. ④ Finally, the failure probability under tensile failure is $p_{ft}=n_t/10^6$, the probability of failure of a pipe under compressive buckling is $p_{fc}=n_c/10^6$.

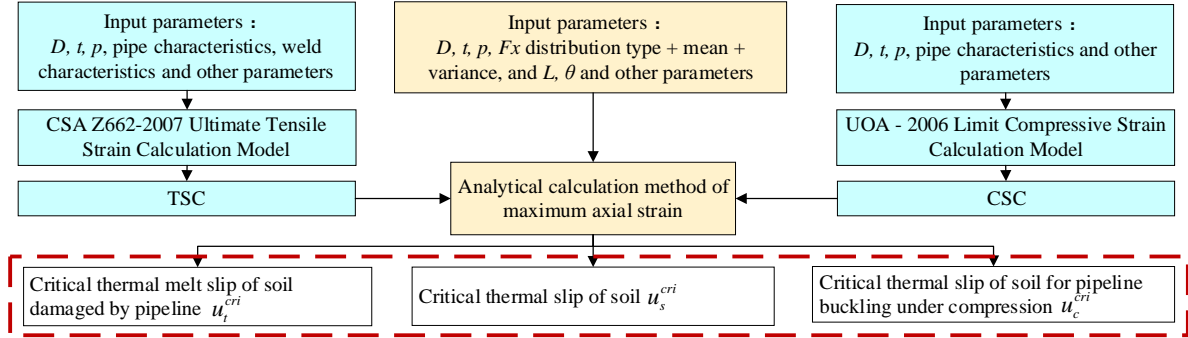


Figure 5: Calculation flow of critical displacements of thawing landslide.

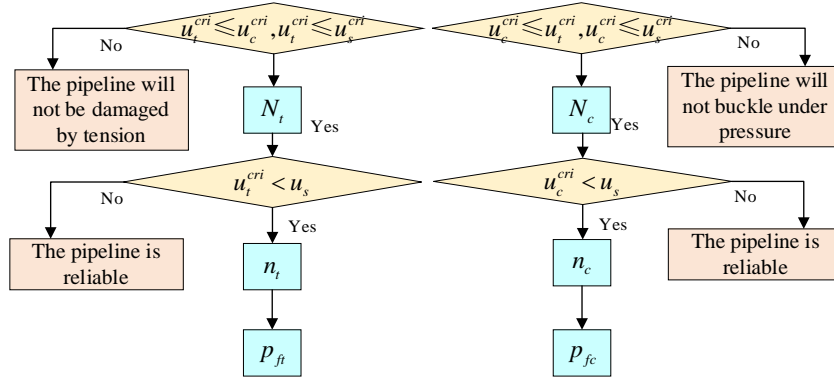


Figure 6: Pipeline failure probability calculation process.

3.2 Model validation

The thermal thawing slip model analyzed with complete independence between wall thickness t , ultimate resistance of soil F_x per unit length, and tensile strength F_y of the pipe, was calculated in agreement with the Zhou.W model [6]. Therefore, the results of the two models using the plot 5 in Zhou.W [6] were selected for comparison and the results are shown in Figure 7. The parameter was set to be consistent with Zhou.W [6], the TSC was taken as 1% and the CSC was used in the UOA model [10], and the other parameters are in that reference [6]. In Figure 7 the difference between the failure probability calculation method of this paper and that of Zhou.W [6] is small, which indicates that the calculation procedure can be adopted.

4 ANALYSIS OF INFLUENCING FACTORS OF STRUCTURAL RELIABILITY OF PIPELINE UNDER THERMAL THAWING SLIP

4.1 Strain capacity of pipes in the analysis of influencing factors

In this study, the yield ratio R_{YT} of the pipe is 0.84 and the apparent toughness δ is 0.3 mm. When analyzing the influencing factors of the tensile failure of the pipe, the ratio of the height of the weld defect to the wall thickness ξ is 0.25; the ratio of the length of the weld defect to the pipe wall thickness η_l is 6.0; the height of the peak-to-valley wave defect on the outer surface of the pipe h_g is taken as 0 mm. When analyzing the influencing factors of the

compressional buckling of the pipe, ζ is 0.20; η_1 is 2.5; h_g is 0.3 mm. thus, the ultimate strain parameters shown in Table 2 are obtained.

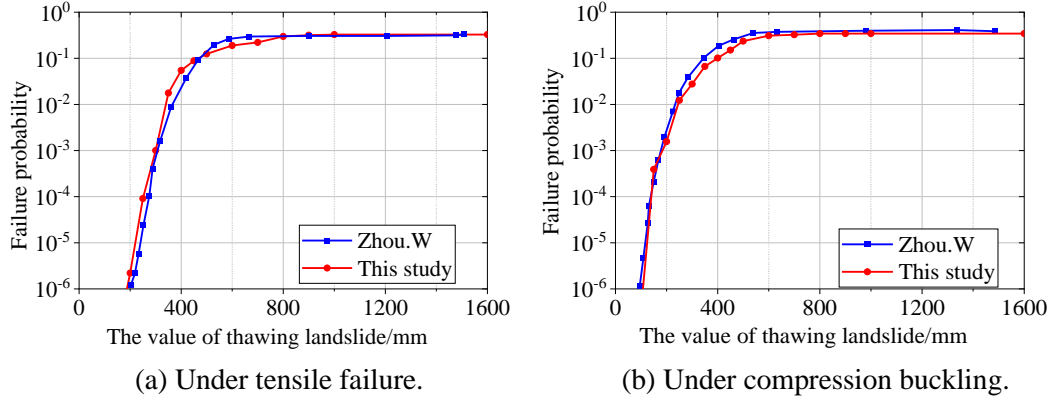


Figure 7: Comparison of pipeline failure probability calculation results.

Table 2: Strain capacity parameter values.

Influencing factors analysis object	R_{YT}	δ (mm)	ζ	η_1	h_g (mm)
Tensile failure	0.84	0.3	0.25	6.0	0.0
Compressional buckling	0.84	0.3	0.30	2.5	0.3

4.2 Analysis of basic working conditions

To select a conservative TSC, the quality of the weld of the pipe is considered to be the upper level, the value of each parameter in the Equation (2) is selected as the average, R_{YT} is 0.84, δ is 0.3 mm, ζ is 0.2; η_1 is 2.5. When selecting a more conservative CSC, h_g is 0.01 mm.

Under the working condition (Table 1), the calculated failure probability is shown in Figure 8. When the thermal thawing slip reaches 400 mm, the pipeline may undergo tensile failure, and when the thermal thawing slip reaches 320 mm, the pipeline may be buckled due to compression. With the increase of thermal thawing slip, the failure probability of pipeline buckling under pressure first reaches 10^{-4} , so the pipeline reliability under tension is higher than that of section under pressure.

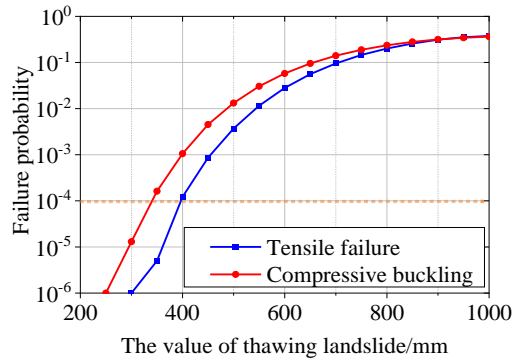


Figure 8: Failure probability of the pipeline under the baseline operating conditions.

4.3 Effect of wall thickness on pipe reliability

Figure 9 shows the relationship between thermal thawing slip and the failure probability with different wall thicknesses. In Figure 9, the design coefficients are taken as 0.4, 0.5, 0.6 and 0.72, while the pipe wall thicknesses correspond to 12.7 mm, 10.3 mm, 8.7 mm and 7.9 mm, the values of other parameters are the same as those in Table 1.

The results in Table 3 show that the smaller the wall thickness of the pipeline makes the critical displacements of thawing landslide smaller and the pipeline reliability lower. Because

the smaller the wall thickness, the greater the hoop stress, which makes the axial strain greater and eventually leads to the axial strain to easily reach the strain capacity of the pipe. Therefore, to ensure the safe operation, the wall thickness can be increased.

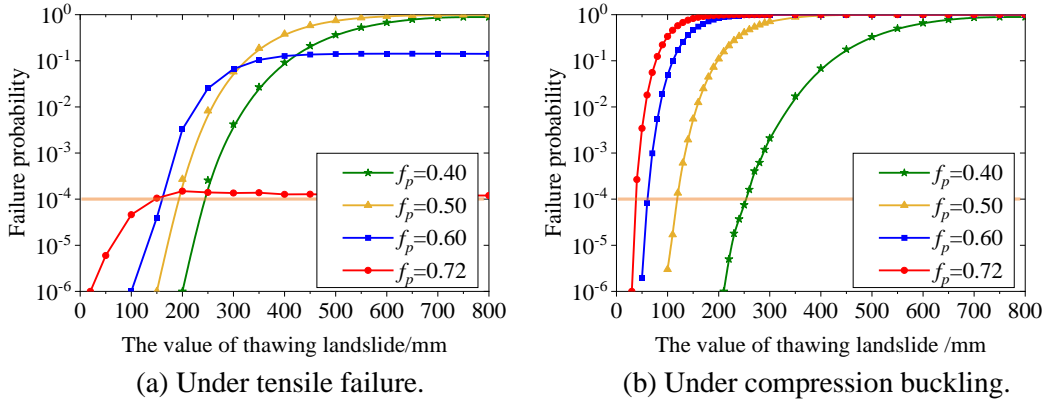


Figure 9: Wall thickness on the probability of failure of the pipe.

Table 3: Strain capacity parameter values.

Wall thickness t (mm)	12.7	10.3	8.7	7.9	
Design factor f_p	0.40	0.50	0.60	0.72	
Critical displacements of thawing landslide u_s (mm)	Under tensile	250	190	150	140
	Under compression	250	120	60	40

4.4 Effect of internal pressure on pipeline reliability

Figure 10 shows the relationship between the thermal thawing slip and the failure probability of pipe with different internal pressures. In Figure 10, the internal pressure is taken as 0 MPa, 5.80 MPa (design factor 0.4), 7.26 MPa (design factor 0.5), 8.71 MPa (design factor 0.6), and 10.45 MPa (design factor 0.72), respectively, and the other parameters are taken as in Table 1.

The results in Table 4 show that the greater the internal pressure makes the critical displacements of thawing landslide smaller and the pipeline reliability lower. Because the higher the internal pressure, the higher the hoop stress, which makes the axial strain greater and eventually leads to the axial strain to easily reach the strain capacity. Therefore, reducing the internal pressure can improve the pipeline reliability.

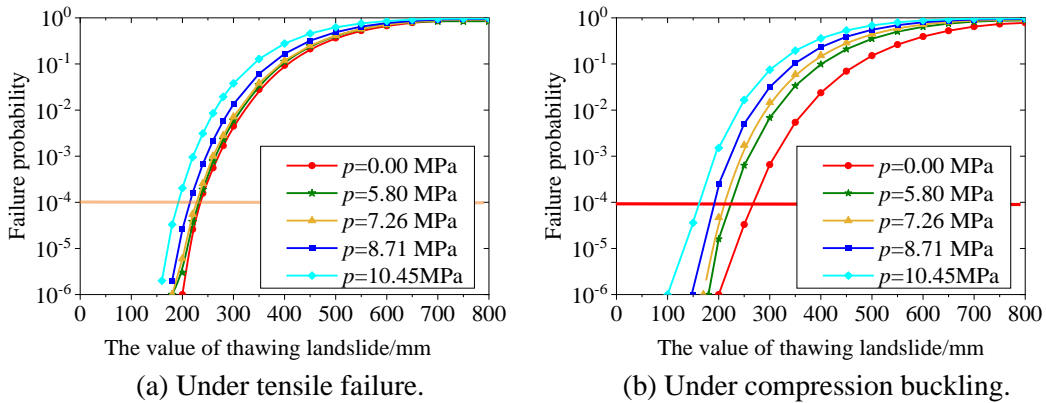


Figure 10: Effect of operating internal pressure on the probability of pipe failure.

Table 4: Strain capacity parameter values.

Operation internal pressure p (MPa)	0	5.80	7.26	8.71	10.45	
Design factor f_p	—	0.4	0.5	0.6	0.72	
Critical displacements of thawing landslide u_s (mm)	Under tensile	230	228	225	220	190
	Under compression	260	210	220	200	150

4.5 Effect of soil ultimate resistance on pipeline reliability

Figure 11 shows the relationship between the amount of thermal thawing slip and the failure probability of pipe under different soil ultimate resistance. In Figure 11, the soil ultimate resistance per unit length is taken as 61.30 N/mm, 76.62 N/mm, 91.95 N/mm, 107.27 N/mm and 122.60 N/mm; the values of other parameters are the same as those in Table 1.

The results in Table 5 show that the greater the soil ultimate resistance makes the critical displacements of thawing landslide smaller, and the lower the reliability of the pipeline. Because the greater the soil ultimate resistance is, the greater the axial frictional effect on the pipe, which makes the axial strain greater and eventually leads to the axial strain to easily reach the strain capacity of the pipe. Therefore, the reliability is influenced by the ultimate resistance of the soil, and the backfilling of the trench with the soil with less ultimate resistance can be used to improve the reliability of the pipeline.

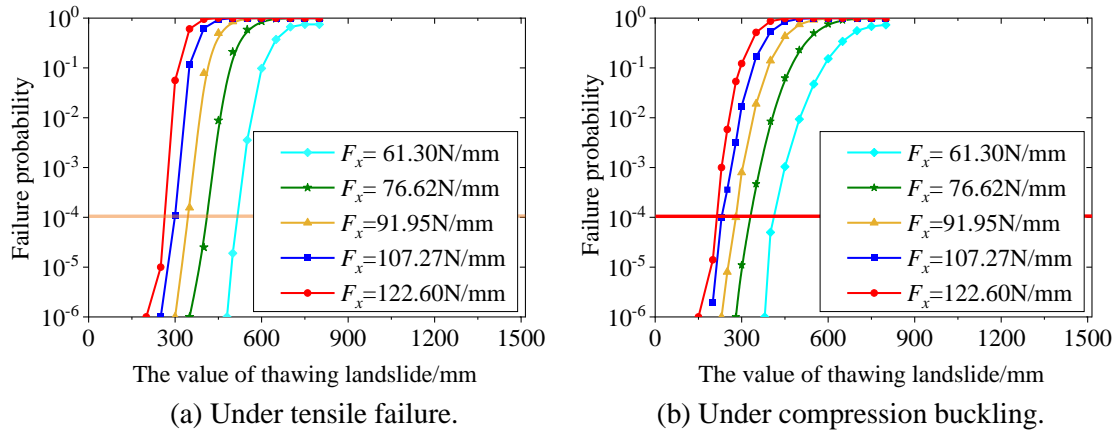


Figure 11: Effect of soil ultimate resistance on the failure probability of pipe.

Table 5: Critical displacements of thawing landslide.

Soil ultimate resistance F_x (N/mm)	61.30	76.62	91.95	107.27	122.60	
Design factor f_p	520	410	350	300	260	
Critical displacements of thawing landslide u_s (mm)	Under tensile	275	230	215	190	190
	Under compression	91.95	107.27	122.60	150	150

5 CONCLUSION

In this paper, the failure probability of pipelines under thermal thawing slip was calculated by Monte Carlo method. First, the ultimate state equation of pipe based on strain is established, the results of the theoretical analysis derived were used to calculate the axial strain. The tensile strain capacity the compressive strain capacity were used to calculated. Next, the failure probabilities of the pipe were calculated by sampling 10^6 times by Monte Carlo method. Finally, the effects wall thickness, internal pressure, and ultimate soil resistance on the pipeline reliability were analyzed, and the critical displacements of thawing landslide was derived based on the ultimate state reliability index of the pipeline in CSA Z662-15 [18].

(1) The greater the wall thickness, the smaller the internal pressure, the smaller the soil ultimate resistance, the greater the critical thermal thawing slip, and the higher the pipeline reliability.

(2) When the ultimate soil resistance decreases, the reliability of the pipeline increases more obviously. Therefore, in engineering applications, compared increasing the wall thickness and reducing internal pressure, the replacement of soil with less friction can improve the pipeline reliability more significantly, thus ensuring a safer pipeline.

REFERENCES

- [1] Wijewickreme D., Honegger D., Mitchell A. and Fitzell T., “Seismic Vulnerability Assessment and Retrofit of a Major Natural Gas Pipeline System: A Case History”, *Earthquake Spectra*, **21**(2), 539-567, 2005.
- [2] Nobahar A., Kenny S., King T., McKenna R. and Phillips R., “Analysis and Design of Buried Pipelines for Ice Gouging Hazard: A Probabilistic Approach”, *Journal of Offshore Mechanics & Arctic Engineering*, **129**(3), 219-228, 2007.
- [3] Alvarado-Franco J.P., Castro D., Estrada N., Caicedo B., Sánchez-Silva M., Camacho L.A. and Muñoz F., “Quantitative-mechanistic model for assessing landslide probability and pipeline failure probability due to landslides”, *Engineering Geology*, **222**, 212-224, 2017.
- [4] Li Y.L., Xu W.B., Chen H.Y., Zeng X.G. and Xu T.L., “Reliability analysis of buried high pressure gas pipeline under the impact of rolling stone”, *China Safety Production Science and Technology*, **08**(4), 29-33, 2012.
- [5] Ma X.L., “Study on the limit state design method of natural gas pipeline under impact external load”, *Southwest Petroleum University*, 2017.
- [6] Zhou W., “Reliability of pressurised pipelines subjected to longitudinal ground movement”, *Structure & Infrastructure Engineering*, **8**(12), 1123-1135, 2012.
- [7] Rajani B.B., Roberson P.K. and Morgenstern N.R. “Simplified design methods for pipelines subjected to transverse and longitudinal soil movements”, *Canadian Geo technical Journal*, **32**, 309-323, 1995.
- [8] Yoosefghodsi N., Zhou J. and Murray D.W., “A Simplified Model for Evaluating Strain Demand in a Pipeline Subjected to Longitudinal Ground Movement”, *International Pipeline Conference*, 2008.
- [9] Canadian Standards Association. Oil and Gas Pipeline Systems. Rexdale, Ontario , Canada,2007.
- [10] Dorey A.B., Cheng J.R. and Murray D.W., “Critical buckling strains in energy pipelines”. *Alberta: University of Albert*, 2001.
- [11] O’rourke M.J, Liu X. and Flores R.B. “Steel pipe wrinkling due to longitudinal permanent ground deformation”, *Journal of Transportaion Rngineering*, **121**(5), 443-451, 1995.
- [12] Wang L.H., Sun P.P., Wu Z.Y., Guo Y. and Wang Q.Y., “Research on reliability-based natural gas pipeline design coefficient”, *Natural Gas and Oil*, **34**(3): 11-14, 2016.
- [13] Yao X.L., Chen H.L., Zhao X., and Guo S.J., “Determination of the weak link of shock resistance of shipboard equipment based on Laida criterion”, *China Ship Research*, **2**(5), 10-14, 2007.
- [14] General Administration of Quality Supervision, Inspection and Quarantine of the People 's Republic of China, GB / T9711-2001.Steel pipe for pipeline system transportation in oil and gas industry.Beijing, *China Quality Inspection Publishing House*, 2001.
- [15] Caleyo F., González J.L. and Hallen J.M, “A study on the reliability assessment methodology for pipelines with active corrosion defects”, *International Journal of Pressure Vessels & Piping*, **79**(1), 77-86, 2002.
- [16] Sun C.M., Li Q., Huang Z.Q., Tang H.P. and Xiao X., “Reliability analysis of corroded pipelines based on Monte Carlo method”, *Oil and gas storage and transportation*, **34**(8), 811-816, 2015.
- [17] Keshtegar, B., Seghier, M. E. A. B., Zhu, S. P., Abbassi, R., and Trung, N. T., “Reliability analysis of corroded pipelines: Novel adaptive conjugate first order reliability method”, *Journal of Loss Prevention in the Process Industries*, **62**, 1-11, 2019.